JOURNAL OF Materials CHEMISTRY

Electroluminescence based on a β-diketonate ternary samarium complex

Youxuan Zheng, Lianshe Fu, Yonghui Zhou, Jiangbo Yu, Yingning Yu, Shubin Wang and Hongjie Zhang

Key Laboratory of Rare Earth Chemistry and Physics, Changchun Institute of Applied Chemistry Chinese Academy of Sciences, Changchun 130022, People's Republic of China. E-mail: yxzheng@ciac.jl.cn or hongjie@ciac.ac.cn

Received 13th November 2001, Accepted 24th January 2002
First published as an Advance Article on the web 5th March 2002

The triplet energy state of the HTH [HTH: 4,4,5,5,6,6,6-heptafluoro-1-(2-thienyl)hexane-1,3-dione] ligand was measured to be 20 400 cm^{-1}, which indicated that $Sm(HTH)_3phen$ (phen: 1,10-phenanthroline) is a good complex to produce strong PL intensity and high fluorescence yield. Electroluminescent (EL) devices using the $Sm(HTH)_3phen$ complex as the emissive center were fabricated by vapor deposition and spin-coating methods. The relative intensity of the EL spectra changed compared to the photoluminescence (PL) spectrum, which suggested that the luminescence mechanisms of PL and EL have differences. A luminance of 9 cd m^{-2} and a higher brightness of 21 cd m^{-2} were obtained from the devices ITO/TPD (40 nm)/$Sm(HTH)_3phen$ (50 nm)/PBD (30 nm)/Al (200 nm) and ITO/PVK (40 nm)/PVK : $Sm(HTH)_3phen$ (2.5 wt%, 50 nm)/PBD (30 nm)/Al (200 nm), respectively.

Introduction

Organic light-emitting diodes (OLEDs) are of great interest because of their efficient emission and their potential application to a new type of full-color-flat-panel display.[1–4] Rare earth complexes have been used as emissive centers in OLEDs in order to improve the color purity of the devices. There are two main advantages for using rare earth materials in OLEDs. One is the very sharp emission of rare earth ions from electronic transitions within the 4f subshells due to the effective shielding by the overlying 5s and 5p orbitals. Another is the possibility of increasing the efficiency of the OLEDs. Generally, the efficiency of OLEDs is limited to 25% by spin statistics as only singlet excitons can recombine to emit light. But when the rare earth complexes are used in OLEDs, the efficiency can reach as high as 100% in theory as both singlet and triplet excitons can transfer their energy to the rare earth ions. Many bright green and red devices with terbium[5–13] and europium complexes[14–25] as emissive centers have been obtained, respectively. Even neodymium,[26–28] ytterbium[29] and erbium[30] complexes have also been applied in the EL study. However, a bright and applied device has not yet been fabricated with rare earth complexes and the OLEDs mechanisms have not been completely understood. Synthesizing new and testing more rare earth complexes of different molecular structures and device architectures will be helpful to improve the device performances and understand the basic EL mechanisms.

Our group has been concentrating on the investigation of the photoluminescent (PL) and electroluminescent (EL) properties of rare earth complexes.[8–12,31] In order to enhance the solubility of the rare earth carboxylate complexes, we introduced a long alkyl chain to the ligands and fabricated several EL devices.[8–11] Additionally, we have observed a 1.5 μm infrared emission in an EL device using an erbium organic complex as the emissive layer.[30]

In this paper, from the low temperature fluorescence spectrum of the gadolinium binary complex $Gd(HTH)_3$ it can be estimated that HTH is a good ligand for the $Sm(HTH)_3phen$ complex to produce strong PL intensity and high fluorescence yield. The $Sm(HTH)_3phen$ complex shows good volatility and solubility in common organic solvents, such as chloroform, acetone, *etc*. Therefore, two types of organic light-emitting diodes (OLEDs) were fabricated by vapor deposition and spin-coating methods using the complex as the emissive center. The variability of the peak intensity in EL spectra compared to the PL spectrum indicates that the luminescence mechanisms of EL and PL have differences.

Experimental

Materials

Samarium oxide (Sm_2O_3, 99.99%) and gadolinium oxide (Gd_2O_3, 99.99%) were purchased from Yue Long Chemical Plant (Shanghai, China). Phen (99.0%, A. R.) and indium tin oxide (ITO) with a sheet resistance of 70 Ω/□ coated glass substrate were purchased from Beijing Chemical Company (Beijing, China) and Guang Ming Glass Company (Shenzhen, China), respectively. HTH, *N*,*N*′-diphenyl-*N*,*N*′-bis(3-methylphenyl)-1,1′-biphenyl-4,4′-diamine (TPD), poly(*N*-vinylcarbazole) (PVK) and 2-(4-biphenyl)-5-(4-*tert*-butylphenyl)-1,3,4-oxadiazole (PBD) were obtained from Aldrich (USA).

Synthesis of complexes

The two rare earth complexes were synthesized by the conventional method described in reference 32: **$Sm(HTH)_3phen$**: Anal. Calcd. for $C_{42}H_{20}O_6S_3F_{21}N_2Sm$ (%): C, 38.98; H, 1.56; O, 7.42; S, 7.43; N, 2.16. Found: C, 38.91; H, 1.59; O, 7.53; S, 7.51; N, 2.04; **$Gd(HTH)_3$**: Anal. Calcd. for $C_{30}H_{12}O_6S_3F_{21}Gd$ (%): C, 32.16; H, 1.07; O, 8.56; S, 8.58. Found: C, 32.06; H, 1.12; O, 8.59; S, 8.62.

To find the melting and decomposition temperature of the Sm-complex, the DSC and TGA were measured as shown in Fig. 1. It can be found that the glass transition temperature of the complex is below 200 °C, but the decomposition temperature is as high as 321 °C. Therefore, the complex did not decompose if we evaporated the Sm-complex at 240 °C.

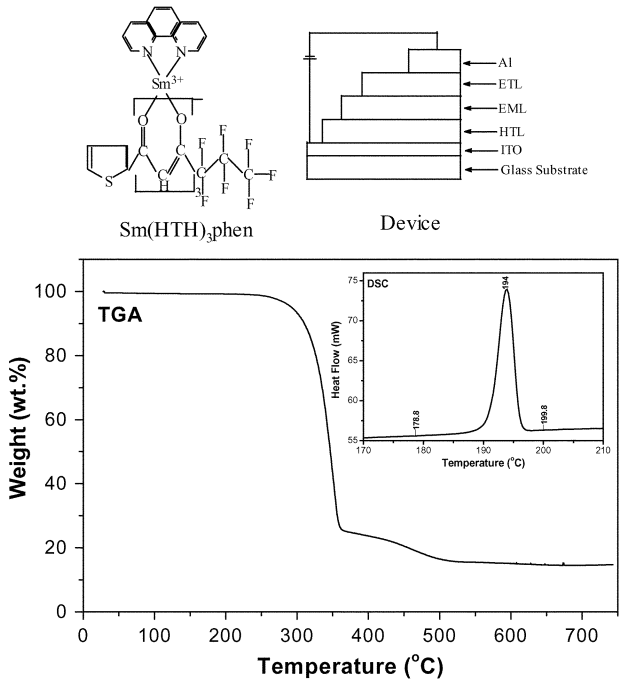

Fig. 1 The device configuration and molecular structure, DSC and TGA curves of the $Sm(HTH)_3phen$ complex.

Preparation of devices

Two types of EL devices with the $Sm(HTH)_3phen$ complex as the emissive center were fabricated by vacuum evaporation (denoted as **EL1**) and spin-coating (denoted as **EL2**) methods, respectively. The device configuration and the molecular structure of $Sm(HTH)_3phen$ are also shown in Fig. 1. The structure of the **EL1** device is ITO/TPD (hole-transporting layer, HTL)/$Sm(HTH)_3phen$ (emitting layer, EML)/PBD (electron-transporting layer, ETL)/Al. All the layers were vapor deposited in a chamber at a pressure under 1×10^{-3} Pa. The deposition rates were maintained to be 0.1 nm s^{-1} for TPD, Sm-complex, PBD and 0.5 nm s^{-1} for Al. The architecture of the **EL2** device is ITO/PVK (HTL)/PVK : $Sm(HTH)_3phen$ (EML)/PBD (ETL)/Al. The HTL and EML were coated in turn by a spin-coating process. Then, a layer of PBD and the Al electrode were deposited on top by vacuum evaporation successively as for **EL1**.

Measurements

The elemental analyses of the samarium and gadolinium complexes were carried out with an Elementar Analysensysteme GmbH VarioEL. The differential scanning calorimetry (DSC) and thermal gravimetric analysis (TGA) were performed on a Perkin–Elmer 7 Series Thermal Analysis System. The low temperature fluorescence spectrum of the $Gd(HTH)_3$ complex was measured on a SPEX 1934D spectrophotometer using a 7 W xenon lamp as the excitation source at liquid nitrogen temperature (77 K). The UV/Vis absorption (ABS) spectrum was measured on a TU-1901 spectrophotometer. The PL and EL spectra were measured with a Shimadzu RF5000 spectrofluorophotometer. The luminance (L)–current density (J) and luminance (L)–voltage (V) curves were obtained from a KEITHLEY2400 SOURCEMETER.

Results and discussion

Fluorescence properties of the HTH ligand at low temperature

Generally, in this rare earth complex, the light of the Sm^{3+} ion emits through the excitation of the ligands. The ligands absorb the energy and are excited to their singlet state, and through intersystem crossing, transit to their triplet state. Then the energy of the singlet and triplet states is intramolecularly transferred to the energy level of the Sm^{3+} ion. Luminescence is emitted when the electron transition to the ground state occurs. In order to determine the triplet energy state of HTH and estimate the suitability of the HTH ligand to the energy level of the Sm^{3+} ion, the low temperature fluorescence spectrum of the $Gd(HTH)_3$ complex (5×10^{-4} M in chloroform solution) was measured at 77 K (Fig. 2). The lowest excited state of Gd^{3+} (^6P) is located at about 32 000 cm^{-1}, which is much higher than the energy of the triplet state of the ligand. Therefore, energy transfer from the ligand to Gd^{3+} is impossible. Thus, the fluorescence spectrum of $Gd(HTH)_3$ is due to the emission of the ligand, and the emission band at the shortest wavelength is assumed to be a 0–0 transition (from the lowest triplet energy state to the ground state of the ligand).[33] In this way, the lowest energy of the triplet state of the ligand can be determined, and the energy difference between the triplet state energy of the organic ligand (Tr) and the resonant level of the Sm^{3+} ion can be calculated [$\Delta E(Tr - E)$]. According to Sato and Wada,[34] intramolecular energy migration efficiency from organic ligands to the central Ln^{3+} is the most important factor influencing the luminescence properties of rare earth complexes. The larger the ΔE is, the lower the luminescence efficiency of the rare earth complexes. From Fig. 2 it can be observed that the shortest fluorescence band emission of the $Gd(HTH)_3$ complex was strong and two clearly-defined peaks can be found. The life time of $Gd(HTH)_3$ is 5.6 ms and the large value indicating the fluorescence comes from the triplet of the HTH ligand. The shortest emission of $Gd(HTH)_3$, assumed to be the 0–0 transition, is 490.2 nm. Therefore, the triplet energy state of HTH is 20 400 cm^{-1}. So, the values of $\Delta E(Tr–{}^4G_{7/2})$, $\Delta E(Tr–{}^4F_{3/2})$ and $\Delta E(Tr–{}^4G_{5/2})$ are 386 cm^{-1} (the energy level of $^4G_{7/2}$ is 20 014 cm^{-1}), 1520 cm^{-1} (the energy level of $^4F_{3/2}$ is 18 832 cm^{-1}) and 2476 cm^{-1} (the energy level of $^4G_{5/2}$ is 17 924 cm^{-1}),[35] respectively. The low different values suggest the intramolecular energy migration efficiency from HTH to the central Sm^{3+} is high and the PL of the $Sm(HTH)_3phen$ complex is strong at room temperature.

Photoluminescence properties of $Sm(HTH)_3phen$

Fig. 3 shows the ABS and PL spectra of the $Sm(HTH)_3phen$ film and the PL spectrum of PVK. It can be found that the ABS spectrum has a wide band with a maximum peak at 340 nm and shoulders at 227 nm and 266 nm. The former (maximum peak) is due to the absorption of the ligand of HTH and the latter (shoulders) is due to the absorption of the second ligand, phen. From the emission spectrum excited by 340 nm it can be observed that the emission spectrum consists of the characteristic emission lines of Sm^{3+}, *i.e.*, $^4G_{5/2} \rightarrow {}^6H_{3/2}$ (532 nm), $^4G_{5/2} \rightarrow {}^6H_{5/2}$ (564 nm), $^4G_{5/2} \rightarrow {}^6H_{7/2}$ (split at 600, 605 and

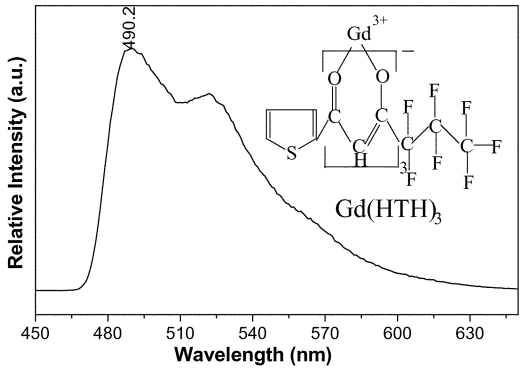

Fig. 2 The fluorescence spectrum of the $Gd(HTH)_3$ complex in chloroform solution (5×10^{-4} M) at 77 K and molecular structure of $Gd(HTH)_3$.

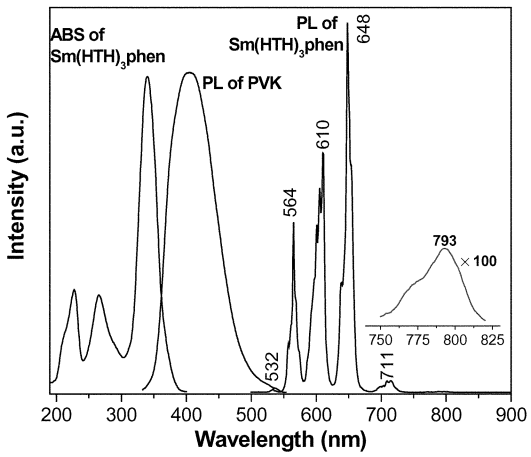

Fig. 3 The ABS, PL spectra of the $Sm(HTH)_3phen$ film and the PL spectrum of PVK.

610 nm), $^4G_{5/2} \rightarrow {}^6H_{9/2}$ (648 nm), $^4G_{5/2} \rightarrow {}^6H_{11/2}$ (711 nm) and $^4G_{5/2} \rightarrow {}^6H_{13/2}$ (793 nm). The intensity sequence of the peaks is $I_{4G5/2 \rightarrow 6H9/2} > I_{4G5/2 \rightarrow 6H7/2} > I_{4G5/2 \rightarrow 6H5/2} > I_{4G5/2 \rightarrow 6H11/2} > I_{4G5/2 \rightarrow 6H3/2} > I_{4G5/2 \rightarrow 6H13/2}$. No emission from the ligands of the complex can be observed. This indicates that a very efficient energy transfer occurs from the ligands to the central Sm^{3+} ion. Generally, in this rare earth complex, the light of the Sm^{3+} ion emits through the excitation of the ligands. As the triplet state energy of ligands increases, the excitation energy is transferred mainly to the higher level. The values of $\Delta E(Tr–G_{7/2})$, $\Delta E(Tr–{}^4F_{3/2})$ and $\Delta E(Tr–{}^4G_{5/2})$ are not great, the energy of the triplet level of HTH can be transferred to the three excited states. It is difficult to observe the emissions of $^4F_{3/2} \rightarrow {}^6H_J$ and $^4G_{7/2} \rightarrow {}^6H_J$ in this Sm-complex though the *Tr* of the ligands is higher than these energy level. The reason is the small energy differences between the $^4F_{3/2}$ and $^4G_{7/2}$ (1182 cm^{-1}), $^4F_{3/2}$ and $^4G_{5/2}$ (2090 cm^{-1}), $^4G_{7/2}$ and $^4G_{5/2}$ (908 cm^{-1}) levels and the rapid non-radiative relaxation *via* phonons to the $^4G_{5/2}$ level. It is easy for the electrons of $^4F_{3/2}$ and $^4G_{7/2}$ levels to relax to the $^4G_{5/2}$ level and only the $^4G_{5/2} \rightarrow {}^6H_J$ transitions can be observed at room temperature.

EL properties of EL1

The EL spectrum of **EL1** ITO/TPD (40 nm)/$Sm(HTH)_3phen$ (50 nm)/PBD (30 nm)/Al (200 nm) can be measured at 8 V (dc) and a luminance of 1 cd m^{-2} was obtained at 10 V, which is defined as the turn-on voltage. The *J–V*, *L–V* and η (efficiency, luminance/current density)–*L* curves of **EL1** are shown in Fig. 4. A maximum luminance of 9 cd m^{-2} was obtained at 21 V (245 mA cm^{-2}) and the efficiency was 0.04 cd A^{-1}. The highest efficiency is 0.07 cd A^{-1} at 14 V (75 mA cm^{-2}). From the $\eta–L$ curve it can be seen that in the low current region, the efficiency increases with increasing current density. The majority of the carriers may be holes because the hole mobility in the TPD layer is higher than the electron mobility in the PBD layer.[36] Since the electric field across the PBD and $Sm(HTH)_3phen$ layers is increased due to the confinement of holes in the TPD layer, electron injection, and consequently, recombination efficiency increases with an increase of the current density. But after reaching its maximum value, the efficiency decreases when increasing the high current density. This can be partly attributed to the quenching of the excited state of the Sm-complex by charge carriers since the concentration of these increases with increased current density.

Fig. 5 shows the EL spectrum of **EL1** at 14 V. It can be observed that the peak positions are identical to that of the PL spectrum. But the relative intensity sequence of peaks (integrated intensity) is changed to $I_{4G5/2 \rightarrow 6H7/2} > I_{4G5/2 \rightarrow 6H5/2} \cong I_{4G5/2 \rightarrow 6H9/2} > I_{4G5/2 \rightarrow 6H11/2} > I_{4G5/2 \rightarrow 6H3/2}$. The highest transition is $^4G_{5/2} \rightarrow {}^6H_{7/2}$, and not $^4G_{5/2} \rightarrow {}^6H_{9/2}$. The peak of $^4G_{5/2} \rightarrow {}^6H_{13/2}$ disappears due to the weak EL emission and the $^4G_{5/2} \rightarrow {}^6H_{7/2}$ transition does not split. These results indicate that the PL and EL luminescence mechanisms have differences. Reference 13 reported the relative intensity change of the $^5D_4 \rightarrow {}^7F_6$ and $^5D_4 \rightarrow {}^7F_5$ transitions of the Tb-complex between the PL and EL spectra, but the reasons need deep investigation. On the Commission Internationale de l'Eclairage (CIE) chromaticity coordinate, the emission of the powder is located in a "orange–red" region ($x = 0.6134$, $y = 0.3609$). The color purity is 82.67% and the red color ratio is $K_r = 0.91$. The ratio of green color is $K_r = 0.70$. But in the emission of **EL1**, the color coordinates are $x = 0.5844$ and $y = 0.3893$. The red and green color ratios are $K_r = 0.85$ and $K_g = 0.14$, respectively.

Optical properties of $Sm(HTH)_3phen$ doped with PVK

From Fig. 3 it can also be observed that the ABS of the $Sm(HTH)_3phen$ complex and the EM spectra have an overlap area. This indicates that the energy can be transferred from PVK to the $Sm(HTH)_3phen$ complex *via* Förster transfer. So, to enhance the optical properties of the samarium complex and the devices, PVK was introduced into the devices. The emissive layer of $Sm(HTH)_3phen$ doped in PVK can not only enhance film-forming and carrier-transporting properties, but can also prevent concentration quenching of the samarium complex. Thus, the injection of the carriers in the EML will be greatly enhanced and a good film can be obtained by the spin-coating method. This method will simplify the fabrication process and avoid the thermal decomposition of luminescent materials caused by evaporation under vacuum. Since the overlap between PVK emission and $Sm(HTH)_3phen$ ABS is significant between 330–400 nm, we conclude that the energy transfer

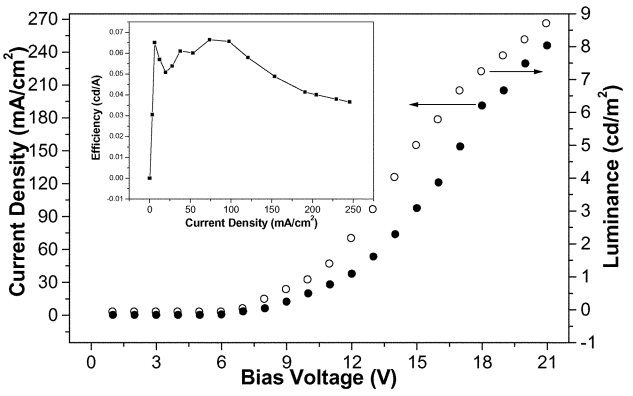

Fig. 4 The *L–J*, *L–V* and $\eta–V$ (insert) curves of the device **EL1** ITO/TPD (40 nm)/$Sm(HTH)_3phen$ (50 nm)/PBD (30 nm)/Al (200 nm).

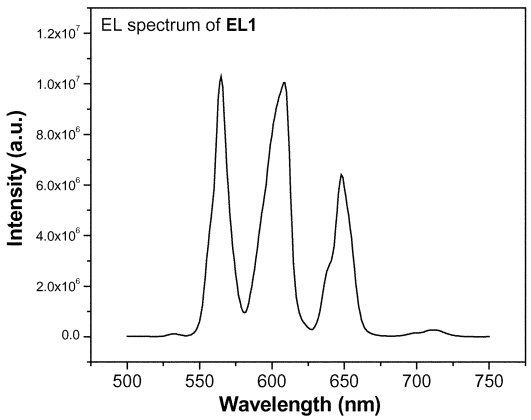

Fig. 5 The EL spectrum of **EL1** at 14 V.

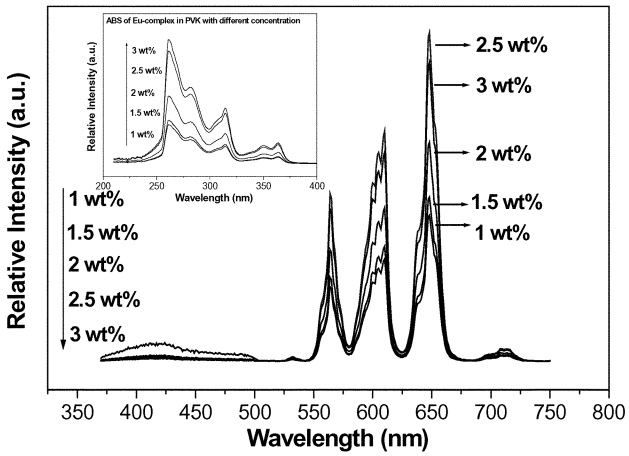

Fig. 6 The ABS (insert) and the PL spectra of the $Sm(HTH)_3phen$ doped in PVK films with different concentrations.

from the PVK to the samarium complex is not very efficient. To quantitatively determine the effectiveness of the $Sm(HTH)_3phen$ complex at accepting energy from PVK, a series of thin films were cast with a different $Sm(HTH)_3phen$ doped concentration in PVK (0.5, 1, 1.5, 2, 2.5, 3 wt%). The emission spectra were measured to determine the best $Sm(HTH)_3phen$ concentration to produce the highest brightness (Fig. 6). When the doped concentrations are lower than 2 wt%, the spectra are composed of both PVK and $Sm(HTH)_3phen$ complex emission. The energy transfer from PVK to $Sm(HTH)_3phen$ is incomplete because the average distance from a photoexcited polymer chain to the nearest Sm complex is too large and the energy transfer is inefficient (so the emission of PVK can also be measured). The PL intensity of the Sm^{3+} ion is enhanced by increasing the $Sm(HTH)_3phen$ dopant concentration in the PVK film, indicating that the degree of energy transfer from PVK to $Sm(HTH)_3phen$ increases with the $Sm(HTH)_3phen$ concentration. When the concentration of $Sm(HTH)_3phen$ is 2.5 wt%, only the emission of $Sm(HTH)_3phen$ can be measured and the PL intensity is highest. At higher dopant concentration, all the energy of PVK is effectively transferred to the $Sm(HTH)_3phen$ complex, but concentration quenching reduces the PL intensity. Thus, the doped concentration of 2.5 wt% is necessary to observe only the emission of the complex when the PL intensity is at its highest. The distance between centers of neighboring complexes is well situated and the $Sm(HTH)_3phen$ complex does not aggregate.

EL properties of EL2

The EL spectrum of the device ITO/PVK (40 nm)/PVK : $Sm(HTH)_3phen$ (2.5 wt%, 50 nm)/PBD (30 nm)/Al (200 nm) is shown in Fig. 7. It shows the characteristic emission of Sm^{3+} ions indicating that the emission only originates from

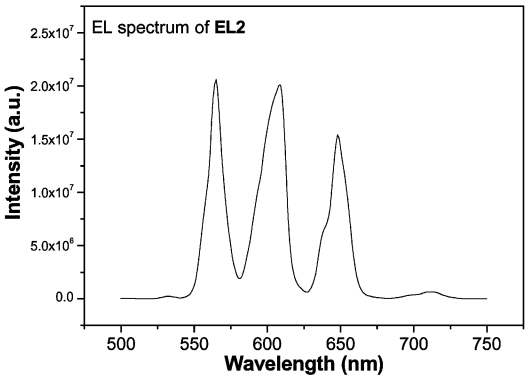

Fig. 7 The EL spectrum of **EL2** at 14 V.

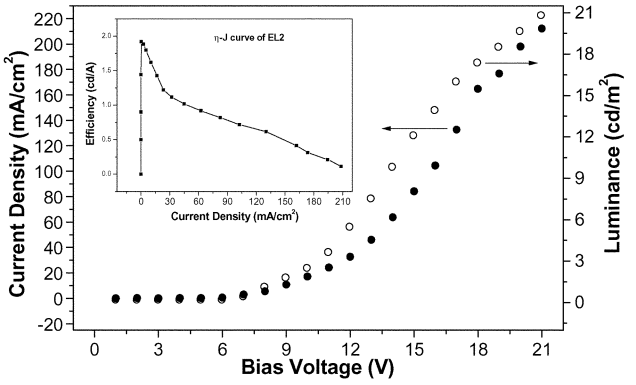

Fig. 8 The *L*–*J*, *L*–*V* and η–*V* (insert) curves of the device **EL2** ITO/PVK (40 nm)/PVK : $Sm(HTH)_3phen$ (2.5 wt%, 50 nm)/PBD (30 nm)/Al (200 nm).

the $Sm(HTH)_3phen$ complex. It can also be assumed that the hole–electron recombination takes place in the blend layer. The relative intensity (integrated intensity) of the peaks have little changes compared to the **EL1** device. The intensity sequence is $I_{4G5/2 \rightarrow 6H7/2} > I_{4G5/2 \rightarrow 6H9/2} > I_{4G5/2 \rightarrow 6H5/2} > I_{4G5/2 \rightarrow 6H11/2} > I_{4G5/2 \rightarrow 6H3/2}$. The excitation mechanism can be explained as energy transfer from the host PVK to the Sm complex. PVK and the ligands of the complex were excited by the hole–electron recombination and free electrons with high energy. Then, the excited state energy of PVK was transferred to the ligands of the Sm-complex. Singlets and triplets that formed on the ligands can be transferred to the Sm^{3+} ion to generate light.

The EL of **EL2** can be measured at 6 V and the turn-on voltage is 9 V. The *J*–*V*, *L*–*V* and η–*L* curves of **EL2** are identical to that of **EL1** in shape (Fig. 8). A maximum luminance of 21 cd m^{-2} was obtained at 21 V (212 mA cm^{-2}, η = 0.114 cd A^{-1}). The higher luminance and efficiency compared to that of **EL1** is due to the introduction of PVK. It is thought that the PVK acts as a hole injection and electron blocking layer and energy transfer to the $Sm(HTH)_3phen$ complex in the EML. In addition, the film-forming and hole-transporting properties of the EML were enhanced.

Conclusion

We have succeeded in obtaining electroluminescence through the use of $Sm(HTH)_3phen$ as the emissive center in triple layered devices. From the difference of the PL and EL spectra it can be concluded that the EL and PL luminescence mechanisms are not the same. A luminance of 9 cd m^{-2} and a higher brightness 21 cd m^{-2} were obtained from the devices ITO/TPD (40 nm)/$Sm(HTH)_3phen$ (50 nm)/PBD (30 nm)/Al (200 nm) and ITO/PVK (40 nm)/PVK : $Sm(HTH)_3phen$ (2.5 wt%, 50 nm)/PBD (30 nm)/Al (200 nm), respectively.

Acknowledgement

"973"- National Key Project for Fundamental Research of Rare Earth Functional Materials of China (No. 29731010) and National Noble Youth Sciences Foundation of China (No. 29225102). National Natural Sciences Foundation of China (No. 20127101, No. 20171043).

References

1 C. W. Tang and S. A. VanSlyke, *Appl. Phys. Lett.*, 1987, **51**, 913.
2 C. Adachi, S. Tokito, T. Tsutsui and S. Saito, *Jpn. J. Appl. Phys.*, 1988, **27**, 269.
3 J. H. Burroughes, D. D. C. Bradley, A. R. Brown, N. Marks, K. Mackay, R. H. Friend, P. L. Burns and A. B. Holmes, *Nature*, 1990, **347**, 539.
4 A. J. Epstein, Y. Z. Wang, S. W. Jessen, J. W. Blatchford,

D. D. Gebler, L. B. Lin, T. L. Gustafson, T. M. Swager and A. G. MacDiarmid, *Polym. Prepr.*, 1996, **37**, 133.
5 J. Kido, K. Nagai and Y. Ohashi, *Chem. Lett.*, 1990, **220**, 657.
6 A. Edwards, C. Claude, I. Sokolik, T. Y. Chu, Y. Okamoto and R. Dorsinvill, *J. Appl. Phys.*, 1997, **82**, 1841.
7 X. C. Gao, H. Cao, C. H. Huang, B. G. Li and S. Umitani, *Appl. Phys, Lett.*, 1998, **12**, 2217.
8 B. Li, D. G. Ma, H. J. Zhang, X. J. Zhao and J. Z. Ni, *Thin Solid Films*, 1998, **325**, 259.
9 D. G. Ma, D. K. Wang, B. Li, Z. Y. Hong, S. Lu, L. X. Wang, N. Minami, N. Takada, Y. Ichino, K. Yase, H. J. Zhang, X. B. Jing and F. S. Wang, *Synth. Met.*, 1999, **102**, 1136.
10 Y. X. Zheng, C. Y. Shi, Y. J. Liang, Q. Lin, C. Guo and H. J. Zhang, *Synth. Met.*, 2000, **14**, 321.
11 Q. Lin, C. Y. Shi, Y. J. Liang, Y. X. Zheng, S. B. Wang and H. J. Zhang, *Synth. Met.*, 2000, **14**, 373.
12 Y. X. Zheng, J. Lin, Y. J. Liang, Q. Lin, Y. N. Yu, Q. G. Meng, Y. H. Zhou, S. B. Wang, H. Y. Wang and H. J. Zhang, *J. Mater. Chem.*, 2001, **10**, 2615.
13 S. Capecchi, O. Renault, D.-G. Moon, M. Halim, M. Etchells, P. J. Dobson, O. V. Salata and V. Christou, *Adv. Mater.*, 2000, **12**, 1591.
14 J. Kido, H. Hagase, K. Hongawa and K. Nagai, *Appl. Phys. Lett.*, 1994, **65**, 2124.
15 T. Sano, M. Fujita, T. Fujii, Y. Hamada, K. Shibata and K. Kuroki, *Jpn. J. Appl. Phys.*, 1995, **34**, 1883.
16 R. A. Campos, I. P. Kovaley, Y. Guo, N. Wakili and T. Skotheim, *J. Appl. Phys.*, 1996, **80**, 7144.
17 K. Okada, M. Uekawa, Y. F. Wang, T. M. Chen and T. Nakaya, *Chem. Lett.*, 1998, 801.
18 M. D. McGehee, T. Bergstedt, C. Zhang, A. P. Saab, M. B. O'Regan, G. C. Bazan, V. I. Srdanov and A. J. Heeger, *Adv. Mater.*, 1999, **11**, 1349.
19 K. Okada, Y. F. Wang, T. M. Chen, M. Kitamura, T. Nakaya and H. Inoue, *J. Mater. Chem.*, 1999, **9**, 3023.
20 C. Adachi, M. A. Baldo and S. R. Forrest, *J. Appl. Phys.*, 2000, **87**, 8049.
21 G. Yu, Y. Q. Liu, X. Wu, D. B. Zhu, H. Y. Li, L. P. Jin and M. Z. Wang, *Chem. Mater.*, 2000, **12**, 2537.
22 M. Iwamuro, T. Adachi, Y. Wada, T. Kitamura and S. Yanagida, *Chem. Lett.*, 1999, 539.
23 O. M. Khreis, R. J. Curry, M. Somerton and W. P. Gillin, *J. Appl. Phys.*, 2000, **87**, 7589.
24 C. J. Liang, D. Zhao, Z. R. Hong, D. X. Zhao, X. Y. Liu, W. L. Li, J. B. Peng, J. Q. Yu, C. S. Lee and S. T. Lee, *Appl. Phys. Lett.*, 2000, **76**, 67.
25 L. Huang, K. Z. Wang, C. H. Huang, F. Y. Li and Y. Y. Huang, *J. Mater. Chem.*, 2001, **11**, 790.
26 M. Iwamuro, T. Adachi, Y. Wada, T. Kitamura and S. Yanagida, *Chem. Lett.*, 1999, 539.
27 Y. Kawamura, Y. Wada, Y. Hasegawa, M. Iwamuro, T. Kitamura and S. Yanagida, *Appl. Phys. Lett.*, 1999, **74**, 3245.
28 O. M. Khreis, R. J. Curry, M. Somerton and W. P. Gillin, *J. Appl. Phys.*, 2000, **88**, 777.
29 Y. Kawamura, Y. Wada, M. Iwamura, T. Kitamura and S. Yanagida, *Chem. Lett.*, 2000, 280.
30 R. G. Sun, Y. Z. Wang, B. B. Zheng, H. J. Zhang and A. J. Epstein, *J. Appl. Phys.*, 2000, **87**, 7589.
31 B. Yan, H. J. Zhang, S. B. Wang and J. Z. Ni, *Mater. Chem. Phys.*, 1997, **51**, 92.
32 L. R. Melby, N. J. Rose, E. Abramson and J. C. Caris, *J. Am.Chem. Soc.*, 1964, **86**, 5117.
33 W. F. Sager, N. Filipescu and F. A. Serafin, *J. Phys. Chem.*, 1965, **69**, 1092.
34 S. Sato and M. Wada, *Bull. Chem. Soc. Jpn.*, 1970, **43**, 1955.
35 *Theory of Rare Earth Spectra (in Chinese)*, ed. S. Y. Zhang, X. Z. Ren, Press of Science and Technology of Jilin Province, Changchun, 1991, p. 165.
36 C. Hosokawa, H. Tokailin, H. Higashi and T. Kusumoto, *Appl. Phys. Lett.*, 1992, **60**, 1220.